从安第斯到冈底斯:从洋-陆俯冲到陆-陆碰撞

许志琴[1)],赵中宝[2)],马绪宣[2)],陈希节[2)],马元[2)]

1) 南京大学地球科学与工程学院,南京,210046; 2) 中国地质科学院地质研究所,北京,100037

内容提要:全球造山系类型主要分为增生型和碰撞型两大类。现今,全球两大巨型造山系的研究表明:环太平洋增生造山系正在经历洋-陆俯冲过程,新特提斯-喜马拉雅碰撞造山系经历过洋-陆俯冲之后又步入陆-陆碰撞阶段。其中,安第斯造山带是东太平洋 Lazaca 大洋板块多阶段向东俯冲在南美大陆之下后形成的以"大洋板块深(陡)-浅(平)俯冲交替、洋岛-地体增生拼贴、碰撞和俯冲型高原隆升"为特征的现代"安第斯岛弧带"和"安第斯-科迪勒拉俯冲型增生造山系"。位于亚洲大陆内部的冈底斯造山系经历了新特提斯洋盆向北俯冲、消减和洋盆闭合以及印度-亚洲碰撞的两重阶段,具体包括早中生代开始的新特提斯"多洋岛"形成和向拉萨地体的多阶段俯冲汇聚,致使洋岛-地体增生碰撞形成冈底斯岩浆弧,继而铸造了晚白垩世的"安第斯型"俯冲增生造山系;在俯冲和碰撞转换阶段发生了岩浆大爆发并形成冈底斯初始高原;而后才进入印度-亚洲陆陆碰撞阶段,形成大规模的 E-W 向逆冲断裂、走滑断裂和 S-N 向裂谷系。因此,安第斯是冈底斯的前半生,冈底斯的今天是安第斯的未来。研究冈底斯的构造演化,特别是早期的构造岩浆活动,必须与安第斯俯冲增生的历史进行对比。

关键词:造山系类型;安第斯造山带;冈底斯造山带

板块构造的聚散经历了从板块离散—大洋形成—洋/陆俯冲到陆/陆汇聚和碰撞造山的过程。以大陆动力学的视野审视全球造山带,造山带的类型主要分为"俯冲型"和"碰撞型"造山系(带),也有的将碰撞之后产生的陆内造山系称之为"陆内型"造山带(Cawood et al., 2009)。在全球现代大规模造山带中,环太平洋俯冲型和特提斯-喜马拉雅碰撞型造山系最为醒目(图1)。从大地构造和板块动力学角度审视亚洲大陆的大型造山带,可以分为中亚造山系、特提斯造山系,以及西太平洋造山系(图1)。从地质历史角度审视中国大陆众多的造山带,诸如天山-兴安造山带、松潘-甘孜造山带、秦岭-大别造山带、羌塘造山带、冈底斯造山带、祁连造山带、昆仑造山带、滇西造山带、喜马拉雅造山带和华南造山带等,发现它们不仅具有不同的物质组成、结构特征、造山类型、造山时限和造山过程,具有造山类型的多样性、造山过程的长寿性、复合型、叠置性以及地体边界物质组成的复杂性;并且具有造山过程中岩浆作用、变质作用、变形样式、深熔作用和成矿作用的依存性和多期性,因此具有造山动力学机制的复杂性(Xu Zhiqin et al., 2016, 2018)。通过前人的研究发现其中大部分造山带经历了俯冲—碰撞两个阶段的复杂造山历史。

造山带研究已经有近200年历史,在板块构造走上大陆动力学发展的今天,对比中国与世界上典型造山带,对于认识和丰富大陆动力学理论具有重要意义。本文聚焦世界典型的两个造山带:与东太平洋板片俯冲相关的南美安第斯俯冲-增生型造山带以及与新特提斯洋俯冲和印度-亚洲陆陆碰撞相关的冈底斯俯冲-碰撞型造山带,以求追寻造山动力学的实质。

1 安第斯山脉的特征及俯冲增生造山过程

位于太平洋东侧和巴西地盾西侧的安第斯山脉是世界上平均海拔第二高的山脉,延伸约8000 km,

注:本文为国家自然科学基金重点项目(编号41430212)、中国地质调查项目(编号DD20160022-01)和南京大学地球科学和工程学院人才基金项目资助的成果。

收稿日期:2019-01-18;改回日期:2019-01-20;网络发表时间:2019-01-21;责任编辑:周健。

作者简介:许志琴,女,1941年生。中国科学院院士,南京大学地球科学与工程学院教授,1987年获法国蒙贝利耶大学构造地质博士学位,长期从事青藏高原和中国造山带研究。Email:3077864156@qq.com。

引用本文:许志琴,赵中宝,马绪宣,陈希节,马元. 2019. 从安第斯到冈底斯:从洋-陆俯冲到陆-陆碰撞. 地质学报, 93(1):1~11, doi: 10.19762/j.cnki.dizhixuebao.2019001.

Xu Zhiqin, Zhao Zhongbao, Ma Xuxuan, Chen Xijie, Ma Yuan. 2019. From Andean orogen to Gangdese orogeny: from ocean continent subduction to continent-continent collision. Acta Geologica Sinica, 93(1): 1~11.

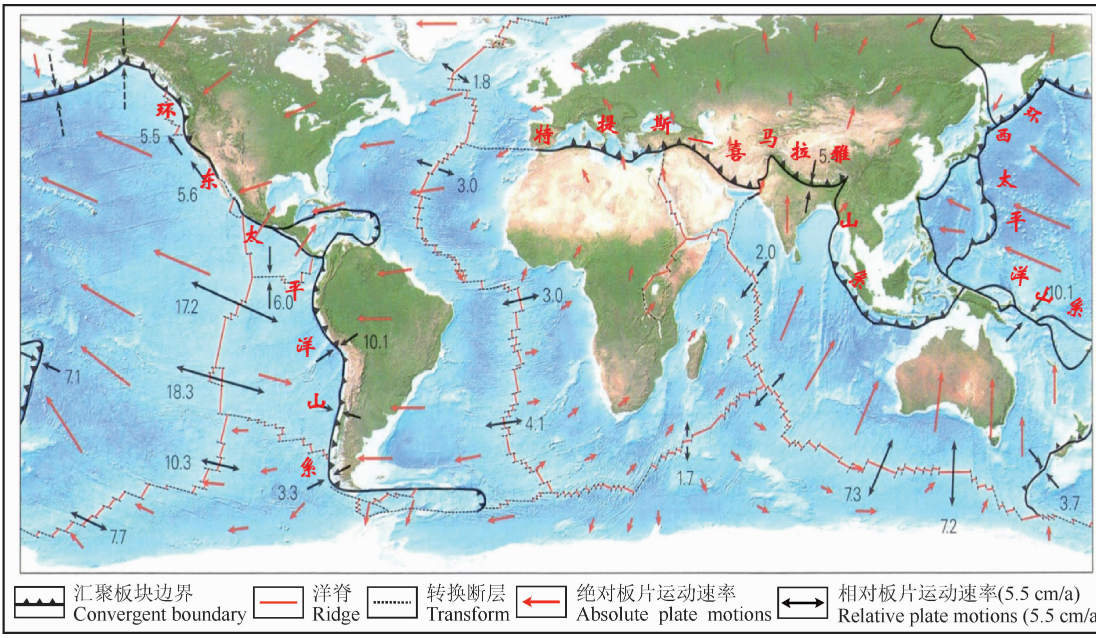

图 1 全球造山带类型示意图(据 Cawood et al., 2009,略加修改)

Fig. 1 Schematic map of the global orogenic belts (modified from Cawood et al., 2009)

图中重点显示了全球现代两大造山系:太平洋周缘的环太平洋山系为增生型山系,特提斯-喜马拉雅山系为碰撞型山系,其经历了洋-陆俯冲到陆-陆碰撞造山过程

The map highlights two major modern orogenic systems on the Earth: around the Pacific Ocean is the accretionary orogenic system, and the Tethys-Himalaya orogenic system is a collisional orogen, which underwent a process from oceanic plate-continental subduction to continent-continental collision

北接加勒比海,南连 Fuego 岛,是南美洲的脊梁(Dewey and Bird, 1970)。安第斯山脉是由于上覆在向东俯冲的太平洋 Nazca 板块之上的南美洲板块西缘在新生代构造缩短而形成的(Sobolev and Babeyko, 2005),与此同时南美洲板块在过去 30 Ma 期间以每百年 2~3cm 的增速向西运动(Silver et al., 1998)。

安第斯山脉的地壳由巨厚的、较热的硅铝质物质组成(Allmendinger et al., 1997; Beck and Zandt, 2002; Yuan et al., 2002)。安第斯山脉的主要构造单元包括"西科迪勒拉山(WC)"、"中安第斯 Altiplano-Puna 高原(AL/PU)"和"东科迪勒拉山(EC)",巴西地盾的西界深入到东科迪勒拉山之中(图 2)。中安第斯高原又被称为 Altiplano-Puna 高原,南北长约 1800 km,东西宽约 200~450 km,平均高度约 4 km,总面积约 500,000 km^2(Isacks, 1988; Barnes and Ehlers, 2009),是世界上的第二高原。

中安第斯高原由于隶属于太平洋洋壳的 Nazca 板块在新生代向东俯冲到南美洲板块之下导致的上地壳缩短(缩短量约 530~150km)而形成的(Isacks, 1988; Allmendinger and Gubbels, 1996; Allmendinger et al., 1997; Lamb et al., 1997; Kley and Monaldi., 1998; Lamb and Davis, 2003; Elger et al., 2005; Sobolev and Babeyko, 2005)。关于中安第斯高原的成因及形成演化现今仍然存在较多的争论(Hartley et al., 2005; Garzione et al., 2006; Hoke and Lamb, 2007; Ehlers and Poulsen, 2009)。一种主流观点认为安第斯高原的形成经历了晚白垩世、晚始新世和晚中新世三次主要的变形事件(MéGard, 1987; de Noblet et al., 1996),其中后两期构造变形事件是由于板块快速汇聚导致(James and Sacks, 1999)。南安第斯和北安第斯地区没有巨大的高原,新生代只经历了约 50 km 的构造缩短(Allmendinger et al., 1997; Lamb et al., 1997; Kley and Monaldi, 1998)。

安第斯山脉是一条近弧形的山脉,根据 Nazca 板块中的洋脊存在和俯冲角度的变化,沿着山脉走向从北向南可以划分以下的地貌-构造省(Rodríguez et al., 2018):

北安第斯地貌-构造省:Nazca 板块 13 Ma 之前形成北火山活动带,13Ma 以来为平俯冲;中安第斯

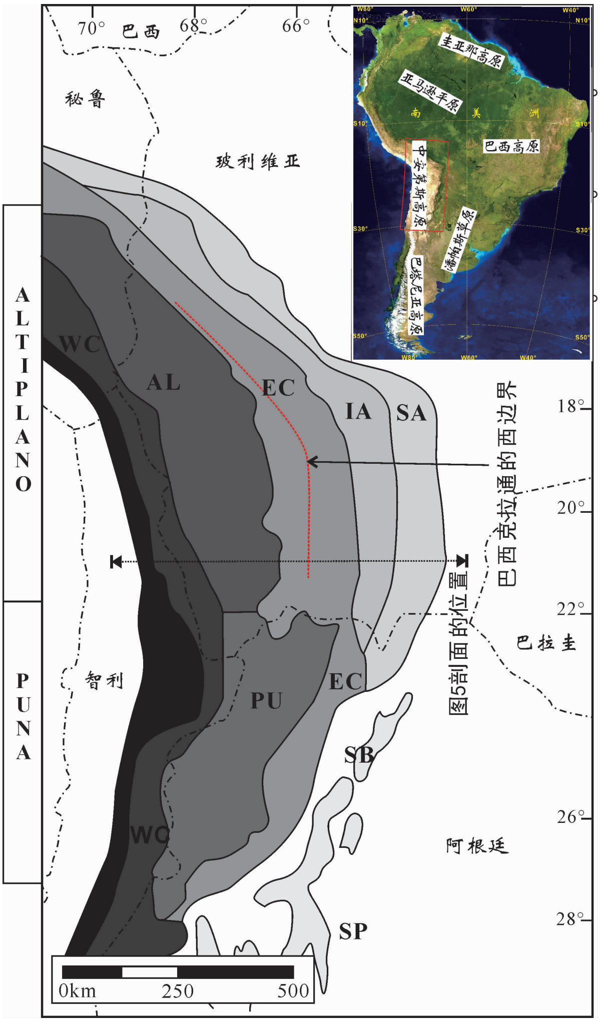

图 2　中安第斯高原地质简图(据 Barnes and Ehlers，2009)

Fig. 2　Geological sketch of the middle Andean Plateau (after Barnes and Ehlers，2009)

WC—科迪勒拉山脉西部；AL/PU—阿尔蒂普拉诺-普纳盆地；EC—科迪勒拉山脉东部；IA—安第斯区域内；SA—次安第斯带；SB—圣巴巴拉山脉；SP—潘佩阿纳斯山脉

WC—western Cordillera；AL/PU—Altiplano-Puna basin；EC—eastern Cordillera；IA—inter Andean zone；SA—Subandes；SB—Santa Barbara Ranges；SP—Sierras Pampeanas

地貌-构造省：位于近 E-W 向 Nazca 洋脊和 Femander 洋脊之间，新生代早期(40Ma)开始，Nazca 板块平俯冲(5°～10°)在南美板块之下，产生 Altiplano 和 Puna 平板域，形成北面的 Altiplano 和南面的 Puna 高原，缺失晚中新世—全新世的火山活动，在两个平板域之间，Nazca 板块陡俯冲(30°)在南美大陆之下，并产生新生代的火山岩；南安第斯地貌-构造省：包含南火山带(图 3)。

安第斯山脉的新生代火山作用开始于西科迪勒拉带(～50 Ma)，并持续到～35 Ma，约 25 Ma 与弧

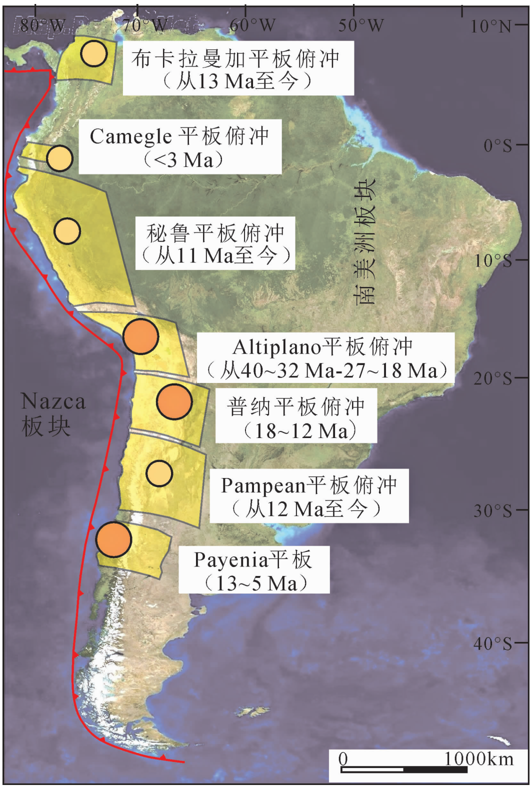

图 3　新生代 Nazca 板块插入南美板块之下的平板俯冲图示(据 Ramos and Folguer，2009)

Fig. 3　Nazaca plate subducted beneath the South American plate as flat slab subduction (modified from Ramos and Folguer，2009)

后拉张有关的铁镁质、流纹质的岩浆作用发育在东西宽约～300 km 的中 Altiplano 高原(Rodríguez et al.，2018)。南纬 ～20°以南的弧岩浆作用有增强的趋势，并且从～12 Ma 开始向南年轻化(Garzione et al.，2016)。强烈的岩浆作用在～3Ma 以来后退到了东西宽～50 km 的西科迪勒拉山，这些岩浆作用可能预示新生代洋壳俯冲角度由正常变为平板俯冲，最后又恢复为正常俯冲(Garzione et al.，2016)。新近纪的拆沉作用可能造成～3 Ma 以来的南安第斯铁镁质岩浆作用，并且在该地区形成了相对于较 Altiplano 高原高的平均海拔(Garzione et al.，2016)。另外，新近纪岩浆作用发育在中安第斯高原的两翼，而上新世—至今的岩浆活动只发育在高原的西翼(Rodríguez et al.，2018)。在南、北安第斯地貌构造省的低角度平板俯冲带几乎不发育新生代火山作用(De Silva.，1989)。

太平洋 Nazca 板块经历了多阶段向东俯冲在南美大陆之下的演化过程(图 4)：①J—K_1(185～130 Ma)：洋内 Amaimer 岛弧形成，Nazca 洋壳板

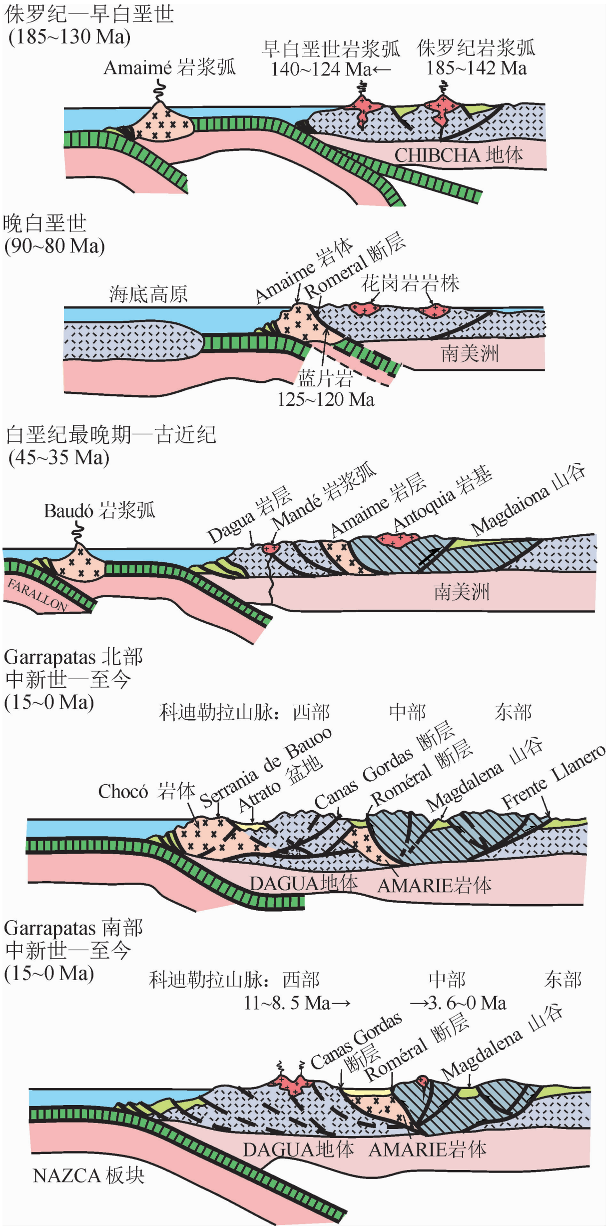

图 4 安第斯俯冲增生造山带的演化模式图

(after Ramos, 2009)

Fig. 4 Geological evolution model for the Andean subduction-accretion orogenic belt

(after Ramos, 2009)

块发生多阶段向东俯冲，在南美大陆西缘形成侏罗纪(185～142 Ma)和早白垩世(140～124 Ma) 岩浆弧组成的安第斯岛弧带；②K_2(90～80 Ma)：大洋中形成洋底高原，Amaime 洋岛地体拼贴在安第斯岛弧带西侧，洋壳俯冲伴随蓝片岩产生；③K_3—E(45～35Ma)：新的 Baudo 洋内弧形成，安第斯岛弧带弧前、弧后的增生，地壳加厚 ；④中新世—现代(15～0 Ma)：Baudo 洋岛地体增生拼贴在安第斯岛弧带西侧，西、中、东科迪勒拉地壳加厚和造山。

2 冈底斯山脉的特征和俯冲-碰撞造山过程

冈底斯造山带(又称冈底斯岩浆弧带)位于喜马拉雅造山系北部和青藏高原南部的拉萨地体之上，全长约 2500 km。西接巴基斯坦北部的 Kohistan-Ladakh 岩浆弧被喀喇昆仑右旋走滑断裂错开(Tapponnier et al., 2001；许志琴等，2012)，东连南迦巴瓦东构造结东南的腾冲岩浆带，拉萨地体北以班公湖-怒江缝合带与羌塘造山带相隔，南以印度斯-雅鲁藏布江缝合带与喜马拉雅造山带毗邻。冈底斯岩浆带具有多期次的强烈岩浆作用，广泛分布的岩浆岩以及东西向分布的斑岩型 Cu-Au 矿化是冈底斯岩浆带的最独特和显著特征，其与沉积作用广泛发育、岩浆作用明显减弱和斑岩成矿作用不明显的拉萨地体中-北部相区分。

冈底斯造山带记录了新特提斯大洋岩石圈板片向北俯冲至亚洲大陆南缘拉萨地体之下，到新生代印度/亚洲陆-陆碰撞造山的过程(Chung et al., 2005；Ji et al., 2009；Zhu et al., 2011, 2015；Ding et al., 2014；Ma et al., 2018)。因此，冈底斯造山带是一个经历洋-陆俯冲增生到陆-陆碰撞造山过程的复合造山带。

冈底斯造山带的构造单元可以分为三部分：三叠纪—白垩纪冈底斯花岗岩基为主的弧岩浆带、白垩纪拉萨弧后盆地和日喀则弧前盆地，以及始新世—中新世冈底斯—造山岩浆岩带(图 6)。冈底斯岩浆带主要由闪长岩、花岗闪长岩、花岗岩以及大量小型辉长岩体组成(Ji et al., 2009；Ma et al., 2018)。冈底斯花岗岩岩基具有 4 个主要阶段的岩浆活动：～230～170 Ma，～110～80 Ma，～65～41 Ma 和～33～10 Ma(Wen et al., 2008；Ji et al., 2009；Wang et al., 2018；Wang et al., 2016)。始新世开始的大规模冈底斯岩浆活动包括 65～43 Ma 的林子宗群火山岩(Mo et al., 2005) 和 69～40 Ma 的曲水岩基(Ji et al., 2009；Ma et al., 2017a；Mo et al., 2005；Wen et al., 2008)，可谓是继中生代冈底斯岩浆事件之后的又一次岩浆大爆发。

三叠纪—白垩纪冈底斯花岗岩浆弧的形成与新特提斯洋岩石圈板块的向北俯冲有关。涉及新特提斯洋盆的早期演化历史尚有争议，研究指出，雄村斑岩 Cu-Au 矿含矿斑岩侵位时间为 167～161Ma 和 181～175Ma(Tafti et al., 2009；唐菊兴等，2010；Lang et al., 2014)。Lang et al. (2014)根据含矿斑

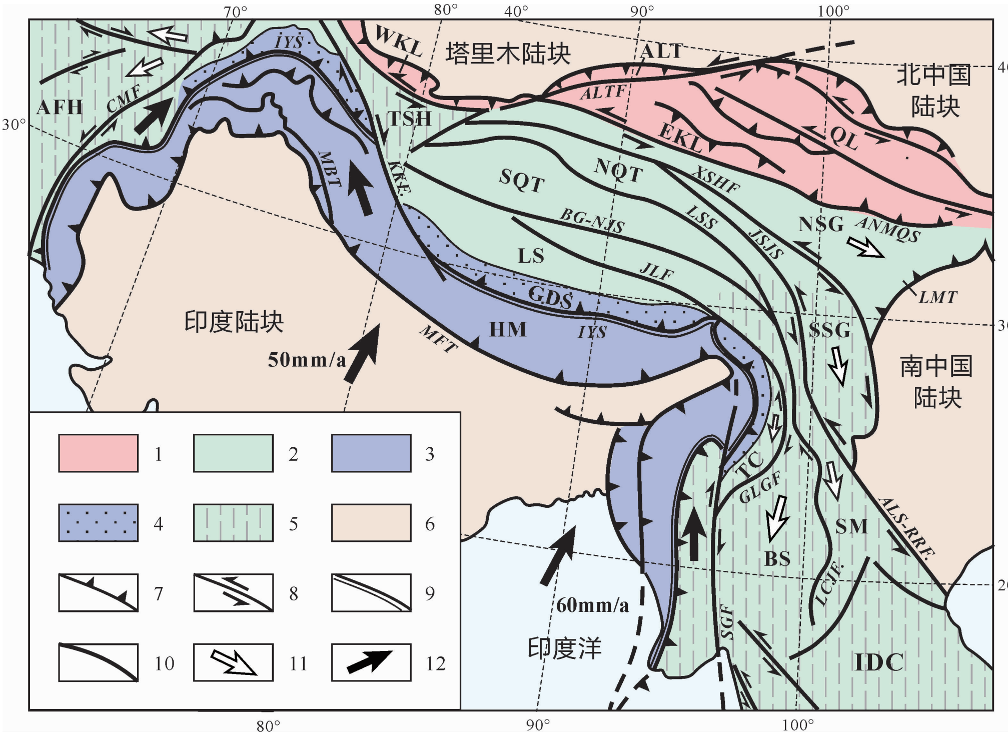

图 5　青藏高原构造构架图(据许志琴等,2016 修改)

Fig. 5　Tectonic framework of the Tibetan plateau and surrounding regions (modified from Xu Zhiqin et al., 2016)

QL—祁连地体;EKL—东昆仑地体;ALT—阿尔金地体;NSG—北松潘-甘孜地体;SSG—南松潘-甘孜地体;NQT—北羌塘地体;SQT—南羌塘地体;WKL—西昆仑地体;TSH—甜水海地体;LS—拉萨地体;TC—腾冲地体;BS—保山地体;SM—思茅地体;IDC—印度支那地体;HM—喜马拉雅地体;AFH—阿富汗地体;GDS—冈底斯地体。ANMQS—阿尼马卿缝合带;JSJS—金沙江缝合带;LSS—龙木错-双湖缝合带;BG-NJS—班公湖-怒江缝合带;IYS—印度-雅鲁藏布江缝合带;ALTF—阿尔金断裂;XSHF—鲜水河断裂;ALS-RRF—哀牢山-红河断裂;LCJF—澜沧江断裂;GLGF—高黎贡断裂;JLF—嘉黎断裂;SGF—实皆断裂;MBT—主边界冲断裂;MFT—主前锋逆冲断裂;KKF—喀喇昆仑断裂;CMF—恰曼断裂。1—始特提斯造山带;2—古特提斯造山带;3—新特提斯造山带;4—新特提斯岩浆带;5—侧向挤出地体;6—邻区陆块;7—逆冲断裂;8—走滑断裂;9—缝合带;10—断裂;11—侧向挤出方向;12—板块运动方向

QL—Qilian terrane; EKL—East Kunlun terrane; ALT—Aljin terrane; NSG—North Songpan Gaze terrane; SSG—South Songpan Gaze terrane; NQT—North Qiangtang terrane; SQT—South Qiangtan terrane; WKL—West Kunlun terrane; TSH—Tianshuihai terrane; LS—Lhasa terrane; TC—Tengchong terrane; BS—Baoshan terrane; SM—Simao terrane; IDC—Indochina terrane; HM—Himalaya terrane; AFH—Afuhan terrane; GDS—Gangdese terrane; ANMQS—Anyemaqen suture; JSJS—Jinshajiang suture; LSS—Longmutso-Shuanghu suture; BG-NJS—Bangonghu-Nujiang suture; IYS—Indus-Tsangbo suture; ALTF—Altyn Tagh fault; XSHF—Xianshuihe fault; ALS-RRF—Ailaoshan-Red River fault; LCJF—Lancangjiang fault; GLGF—Gaoligong fault; JLF—Jiali fault; SGF—Sagaing fault; MBT—Main Bounded fault; MFT—Main frontal fault; KKF—Karakunrun fault; CMF—Chaman fault. 1—Proto-Tethys orogen; 2—Paleo-Tethys orogen; 3—Neo-Tethys orogen; 4—Neo-Tethys magmatic belt; 5—lateral extrusion terrane; 6—adjacent block; 7—thrust; 8—strike-slip fault; 9—suture zone; 10—fault; 11—lateral extrusion direction; 12—moving direction of plate

岩全岩 Nd 值和锆石 Hf 分析结果推测雄村矿形成于早期新特提斯洋内岛弧背景,类似于现今的西南太平洋岛弧(Kesler, 1973; Cooke et al., 1998)。

最近新的研究揭示冈底斯曲水堆晶富闪深成岩岩体岩石地球化学特征与洋内岛弧火山岩有亲缘性,全岩和矿物同位素显示非常亏损的特征,推测 220 Ma 形成的富闪深成岩处在新特提斯洋内俯冲岛弧环境(Ma et al., in press)。

冈底斯造山带的俯冲增生造山作用表现为白垩纪弧后和弧前盆地沉积地层遭受强烈的地壳缩短和加厚,形成以"褶皱-断裂和自北向南剪切的基底滑脱"为特征的拉萨弧后盆地变形(Ma Yuan et al., 2017),以及以"扇形褶皱-断裂系"为特征的日喀则弧前盆地变形(Wang et al., 2017),在大约 90~62 Ma 期间,新特提斯洋向北俯冲引发的地壳缩短和加厚的冈底斯增生造山之后,又经历了山体隆升-剥蚀和构造地貌的削平阶段,并被 69~40 Ma 花岗岩侵入和 65~43 Ma 的大面积近水平的林子宗群火山岩席不整合覆盖,形成冈底斯初始高原(Ma Yuan et al., 2017),由此表明冈底斯俯冲-增生造山向陆-

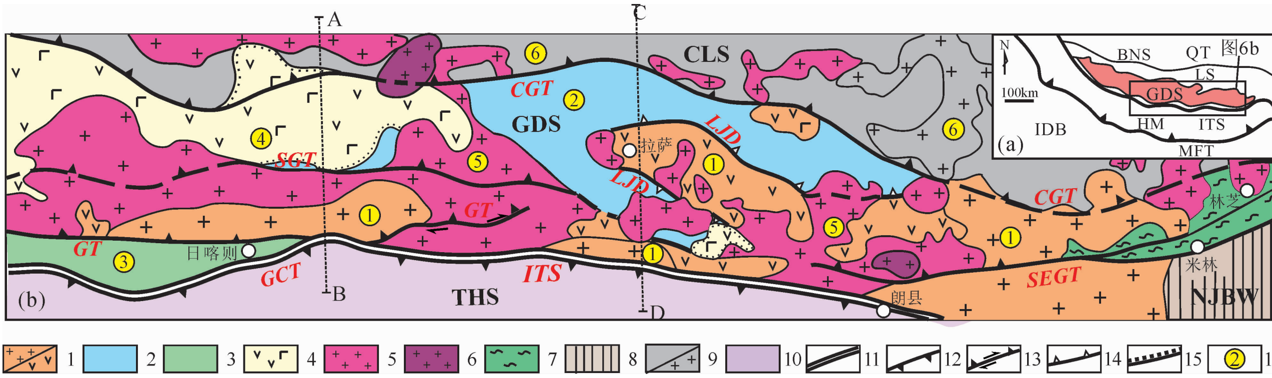

图 6 冈底斯中东段地质构造简图

Fig. 6 Simplified geological structure map of the middle-eastern Gangdese belt

1—中生代岩浆带；2—白垩纪弧后盆地；3—白垩纪弧前盆地；4—林之宗火山岩(65～45 Ma)；5—花岗岩(65～40 Ma)；6～38 Ma 以来的花岗岩；7—高级变质杂岩；8—南迦巴瓦变质杂岩；9—松多印支造山带；10—喜马拉雅地体；11—缝合带；12—逆冲断层；13—走滑断裂；14—拆离断层；15—不整合；16—构造单元

1—Mesozoic magmatic belt; 2—Cretaceous back-arc basin; 3—Cretaceous fore-arc basin; 4—Linzizong volcanic rocks (65～45 Ma); 5—granite (65～40 Ma); 6—granite since 38 Ma; 7—high grade metamorphic complex; 8—Namche Barwa metamorphic complex; 9—Sumdo-Indochina orogenic belt; 10—Himalayan terrane; 11—suture zone; 12—thrusts; 13—strike-slip fault; 14—detachment fault; 15—unconformity; 16—tectonic unit

陆碰撞造山转换的阶段，引发大规模岩浆爆发以及导致冈底斯初始高原的形成，是冈底斯造山带的一个重要特征。

印度-亚洲陆陆碰撞，特别是 40 Ma 以来，近 E-W 走向并向北倾的逆冲断裂系、走滑断裂系和近 N-S 向裂谷系为代表的陆内断裂体系叠置在冈底斯俯冲增生造山带上。在南北向挤压、东西向伸展塌陷作用以及嘉黎-高黎贡右行走滑断裂的(32～21 Ma) 制约下，冈底斯带的物质向东及南东逃逸，并伴随大规模碰撞成矿作用(Hou et al., 2015; Lu et al., 2015; Yang et al., 2015)。～18 Ma 以来冈底斯南缘南倾的大反冲断裂(GCT) (Li et al., 2018) 使得特提斯-喜马拉雅地体向北倒覆在冈底斯造山带之上。

冈底斯造山带经历了如下的构造演化过程(图 7)：

(1)早中生代—白垩纪：新特提斯洋岩石圈板片的多阶段的洋内俯冲以及俯冲洋壳下插于亚洲大陆南缘拉萨地体之下，形成中生代洋内弧岩浆岩和中生代活动大陆边缘岩浆弧、白垩纪弧后和弧前盆地(Ma et al., 2017b; Ma et al., 2018; McDermid et al., 2002; Wang J G et al., 2017; Ziabrev et al., 2004)。

(2)90～65 Ma：白垩纪弧后和弧前盆地沉积地层的强烈褶皱-断裂及基底滑脱造成冈底斯地壳的缩短和加厚，冈底斯俯冲增生造山带形成以及山脉的隆升、剥蚀和削平(Ding et al., 2005; Wang et al., 2017; Ma Yuan et al., 2017)。

(3)65～40 Ma：新特提斯洋盆俯冲到亚洲-印度陆陆碰撞的转换阶段，大规模火山爆发，林子宗火山岩呈近水平岩席不整合覆盖在冈底斯俯冲增生褶皱造山带之上，形成古新世的冈底斯高原，与此同时发育了大范围花岗岩浆侵位(Ding et al., 2003; Mo et al., 2003; Wen et al., 2008; Ji et al., 2009; Lee et al., 2009; Wang et al., 2015; Zhu et al., 2015)。

(4)40 Ma 以来：陆-陆碰撞导致的陆内变形使冈底斯高原遭受进一步南北向挤压，东西向伸展垮塌以及沿走滑断裂物质向东(或南东向)的逃逸(Yin and Harrison, 2000; Tapponnier et al., 2001; Xu et al., 2013)。

3 讨论：安第斯和冈底斯造山带的对比

3.1 大洋板片的俯冲时限

安第斯俯冲增生造山和冈底斯早期的俯冲增生造山分别与太平洋和特提斯洋岩石圈板片分别向东和向北俯冲消减有关。研究表明，两大洋的俯冲起始时间大致相似(早中生代)，但是冈底斯俯冲增生造山历时约 180 Ma(Ao et al., 2018; Ma et al., 2018; Meng et al., 2018; van Hinsbergen et al., 2018; C Wang et al., 2018)，而太平洋板块

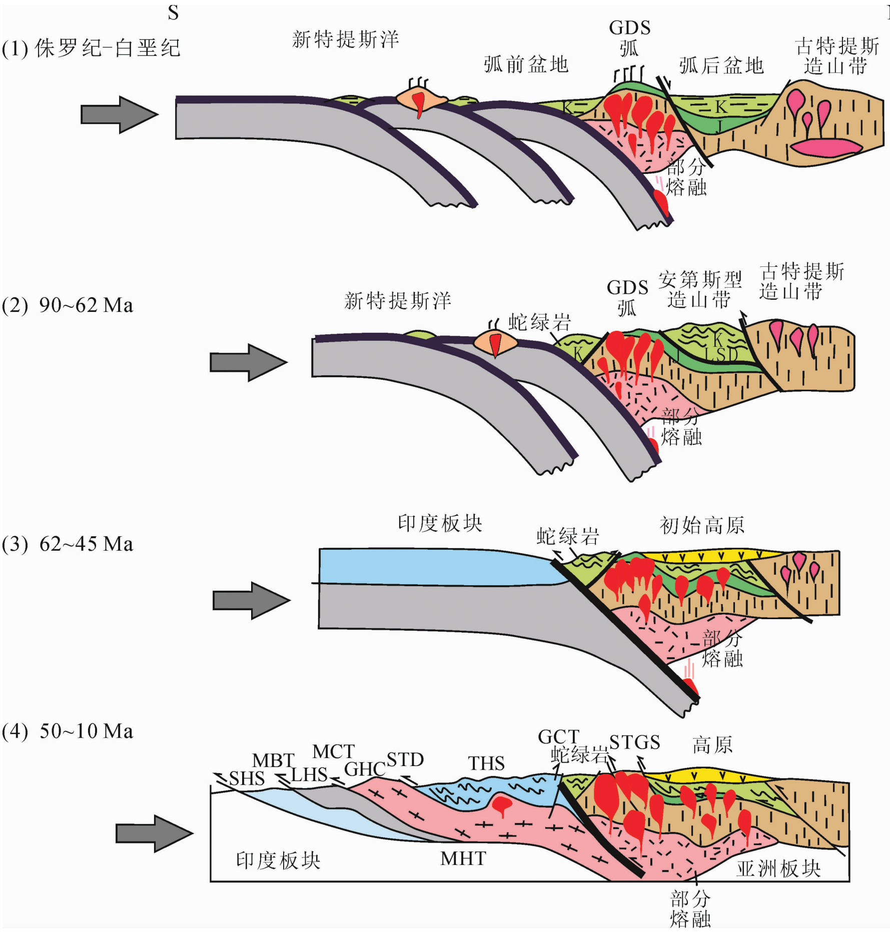

图 7　冈底斯俯冲-碰撞型山脉的构造演化示意图

Fig. 7　A sketch of tectonic evolution of the Gangdese subduction-collisional belt

SHS—次喜马拉雅；LHS—低喜马拉雅；GHC—高喜马拉雅；THS—特提斯喜马拉雅；MBT—主边缘逆冲断裂；MCT—主中央逆冲断裂；STD—藏南拆离系；GCT—大反冲断裂带；GDS—冈底斯；SGTS—南冈底斯逆冲断层系；MHT—喜马拉雅主断层

SHS—Sub Himalaya; LHS—Lower Himalaya; GHC—Great Himalaya; THS—Tethys Himalaya; MBT—Main Boundary thrust; MCT—Main Central thrust; STD—southern Tibet detachment; GCT—Great Counter thrust; GDS—Gangdese arc; SGTS—South Gandese thrust system; MHT—Main Himalaya thrust

向东俯冲造成的安第斯俯冲增生造山至今仍在继续。

3.2　洋岛发育与多阶段洋内俯冲和洋-陆拼贴

重塑安第斯俯冲增生造山过程，发现安第斯山脉自晚白垩世以来先后拼贴了 Ameime，Mande 和 Bauda 火山弧组成的洋岛地体，表明太平洋中曾经存在晚侏罗世—古新世的多期洋内岛弧，继后与南美大陆边缘逐渐拼贴和多次碰撞（Ramos，2009）。近期研究表明，冈底斯中生代俯冲增生造山带中也存在大洋岛弧地体，推测其与安第斯一样，曾发生过多次洋内俯冲以及后续的多次洋-陆拼贴和碰撞（Aitchison et al.，2000；Dai et al.，2011；Ma et al.，2017b；Lang et al.，2018；Ma et al.，2018）。然而，冈底斯早期的俯冲增生历史的重塑要比安第斯山脉要困难的多。

3.3　安第斯与冈底斯山脉的前身

南美安第斯俯冲增生造山带的基底为克拉通基底，包括如下记录：罗迪尼亚汇聚事件（1100 Ma）、泛非事件（520～500 Ma）、冈瓦纳大陆边缘早古生代（480～400 Ma）和晚古生代（300～275 Ma）被动陆缘地台型沉积俯冲到劳亚大陆之下（e.g.，Garzione et al.，2016）。

冈底斯山脉的基底为中拉萨古特提斯造山带基底，含有古特提斯高压变质带（270 Ma）、蛇绿岩（320 Ma）和弧火山岩（C—P）和弧花岗岩浆岩（300 Ma）以及印支造山的变形（240～210 Ma）和岩浆作用（220～190Ma），以及榴辉岩退变质作用（220～200）（Yang et al.，2009；Guo et al.，2016；Zhang et al.，2018；Wang et al.，2019）。因此，安第斯和冈底斯山脉的基底具有本质区别。

3.4 安第斯高原和冈底斯高原

安第斯山脉中发育"中安第斯高原",无独有偶,冈底斯山脉中也发育冈底斯高原,前者为"俯冲型高原",是建立在太平洋板块俯冲于南美大陆西缘地壳之上,引发强烈缩短变形形成的中安第斯山脉,而后者是建立在早期的新特提斯洋壳俯冲造山型高原基础之上,并在印度-亚洲陆陆碰撞之后最终定型的"碰撞型高原"。高原的形成均受控于岩石圈和地壳的特殊结构,并且导致了一系列的变形折返、隆升和岩浆等效应(Barnes and Ehlers, 2009)。

3.5 造山带弧形几何学与板块运动几何学之间的关系

安第斯造山带和冈底斯造山带沿走向均呈现弧形几何学状态,前者的形成与太平洋板片向东俯冲在南美板块之下的角度变化有关,后者与新特提斯大洋板片俯冲和印度/亚洲碰撞的几何学相关。

安第斯山脉的弧形几何学与 Nazca 板块的俯冲几何学密切相关,地球物理结果揭示了 13 Ma 之前 Nazca 板块向东平俯冲在中安第斯高原之下,而其它南、北地区则为较晚的 13 Ma 以来的平俯冲,以此解释了 13 Ma 之前中安第斯山高原形成与平俯冲有关(Ramos and Folguera, 2009; Rodríguez et al., 2018)。而且,中安第斯是山脉弧度向东最突出之处,意味安第斯山脉构造缩短的最大处(图 3)。研究表明,大洋板块俯冲角度几何学是沿着不同地段和不同时期发生变化的。

安第斯高原的形成和太平洋洋壳板片俯冲角度变化的关系如下(Ramos and Folguera, 2009):

(1)在约 25~30Ma 之前,由于大洋俯冲带的平俯冲,导致了俯冲楔上部中安第斯物质的热软化和在挤压背景下强烈的构造缩短(Isacks, 1988),因此开始于古新世(约 60~40M)的安第斯高原,是一个稳定慢速的隆升过程(McQuarrie et al., 2005);而在 25 Ma 开始俯冲角度变陡。

(2)Nazca 板块与南美板块汇聚速率在约 25~30Ma 开始增加(Pardo-Casas and Molnar, 1987),这可以解释安第斯高原在 30~25Ma 之后的快速隆升,高原从约 1km 的高度开始抬升,在约 10~6Ma 时期中安第斯高原快速抬升了约 2.5km(Garzione et al., 2006),在这个阶段俯冲板片的角度逐步变缓。

(3)中安第斯高原形成最重要的先决条件是岩石圈的软化,部分熔融的发生、显著的地幔热对流和加厚地壳的放射热降低了地壳的粘度系数,并使之发生了流动(Royden, 1996; Beaumont et a1., 2001; Vietor and Oncken, 2005)。俯冲的洋壳脱水导致地幔楔的重熔和地幔楔底部碎片化的拆沉,并形成地幔楔的角流,同时俯冲 Nazca 板片的后撤有利于地幔楔顶部地壳的缩短和加厚(McQuarrie et al., 2005)。地壳的缩短导致了厚的、热的长英质的大陆地壳的形成(Allmendinger et al., 1997; Beck and Zandt, 2002)。

(4)新生代气候的变化使得中安第斯海沟饥饿,从而导致 Nazca 板块和南美板块接触部位的强烈剪切应力导致了造山作用及高原形成(Lamb and Davis, 2003)。

冈底斯山脉的几何学与板块运动两重性(俯冲+碰撞)的几何学有关。穿越青藏高原南部的地球物理资料显示两种不同俯冲几何学类型:印度板块俯冲前缘在青藏高原西部平俯冲抵达班公湖-怒江缝合带(地震层析剖面,Guo et al., 2018)和印度板块俯冲前缘呈现陡俯冲可能停滞在印度-亚洲板块边界—印度-雅鲁藏布江缝合带(地震反射剖面,Gao et a1., 2016)。这些地球物理信息反映了大约自陆-陆碰撞以来青藏南部岩石圈地幔和地壳结构的信息,同时地球物理的资料也显示冈底斯地壳的中东段具有低密度和低波速的下地壳物性(Gao et al., 2016),推测冈底斯地体中下地壳流的存在,解释了冈底斯地体中物质大量向东逃逸的根由。但是无疑,现代地球物理结果掩盖了中生代新特提斯大洋岩石圈板块俯冲几何学的信息。

基于以上讨论,通过与安第斯山脉对比,冈底斯山脉在俯冲增生阶段的洋壳板块俯冲几何学可以做如下的推测:①200~100 Ma 新特提斯大洋岩石圈板片的陡俯冲造成拉萨地体南缘大规模岩浆弧发育,由于后期抬升,花岗岩基上隆于地壳浅部,火山弧被大部剥蚀;②冈底斯山脉中部白垩纪(100~65 Ma)弧后和弧前盆地的发育以及地壳缩短造山,该造山作用可能与此时大洋俯冲板块转为"平俯冲"有关,弧后盆地中的滑脱构造可能归因于平俯冲造成的地壳解耦;③65~40 Ma 的大规模岩浆爆发推测与陆陆碰撞引起平俯冲板块的拆沉有关;④40~30 Ma 以来冈底斯山脉的深部结构如同以上提到的地球物理结果所示。

References

Aitchison J C, Badengzhu A M, Davis J B, Liu H, Luo J G, Malpas I R C, McDermid H Y, Wu S V, Ziabrev and Zhou M F. 2000. Remnants of a Cretaceous intra-oceanic subduction system within the Yarlung-Zangbo suture (southern Tibet). Earth and Planetary Science Letters, 183: 231～244.

Allmendinger R W, Jordan T E, Kay S M, Isacks B L. 1997. The evolution of the Altiplano-Puna plateau of the Central Andes. Annual Review of Earth and Planetary Sciences, 25: 139～174.

Allmendinger R W, Gubbels T. 1996. Pure and simple shear plateau uplift, Altiplano-Puna, Argentina and Bolivia. Tectonophysics, 259(1-3): 0～13.

Ao S J, Xiao W J, Windley B F, Zhang J E, Zhang Z, Yang L, and Liu Y. 2018. Components and structures of the eastern Tethyan Himalayan sequence in SW China: Not a passive margin shelf but a mélange accretionary prism. Geological Journal, 53: 2665～2689.

Barnes J B, Ehlers T A. 2009. End member models for Andean Plateau uplift. Earth Science Reviews, 97(1-4): 105～132.

Beaumont C, Jamieson R A, Nguyen M H, Lee B. 2001. Himalayan tectonics explained by extrusion of a low-viscosity crustal channel coupled to focused surface denudation. Nature, 414: 738～742.

Beck S L, Zandt G. 2002. The nature of orogenic crust in the central Andes. Journal of Geophysical Research: Solid Earth, 107(B10).

Cawood P A, Kronre A. 2009. Earth Accretionary Systems in Space and Time. Geological Society, London, Special Publications, 318.

Chung S L, Chu M F, Zhang Y, Xie Y, Lo C H, Lee T Y, Lan C Y, Li X, Zhang Q, Wang Y. 2005. Tibetan tectonic evolution inferred from spatial and temporal variations in post-collisional magmatism. Earth-Science Reviews, 68(3-4): 173～196.

Dai J G, Wang C S, Hébert R M, Santosh Y Li L and Xu J Y. 2011. Petrology and geochemistry of peridotites in the Zhongba ophiolite, Yarlung Zangbo suture zone: Implications for the Early Cretaceous intra-oceanic subduction zone within the Neo-Tethys. Chemical Geology, 288: 133～148.

de Silva S L. 1989. Altiplano-Puna volcanic complex of the central Andes. Geology, 17(12): 1102～1106.

Dewey J F, Bird J M. 1970. Mountain belts and the new global tectonics. Journal of Geophysical Research, 75(14): 2625～2647.

Ding L, Kapp P, Wan X Q. 2005. Paleocene-Eocene record of ophiolite obduction and initial India-Asia collision, south central Tibet. Tectonics, 24, TC3001.

Ding L, Kapp P, Zhong D L, Deng W M. 2003. Cenozoic volcanism in Tibet: Evidence for a transition from oceanic to continental subduction. Journal of Petrology, 44: 1833～1865.

Ding L, Xu Q, Yue Y, Wang H, Cai F, and Li S. 2014. The Andean-type Gangdese Mountains: Paleoelevation record from the Paleocene-Eocene Linzhou basin. Earth and Planetary Science Letters, 392: 250～264.

Ehlers T A, Poulsen C J. 2009. Influence of Andean uplift on climate and paleoaltimetry estimates. Earth and Planetary Science Letters, 281(3-4): 238～ 248.

Elger K, Oncken O, Glodny J. 2005. Plateau-style accumulation of deformation: The southern Altiplano. Tectonics, 24(4): 1～19.

Gao R, Lu Z, Klemperer S L, Wang H, Dong S, Li W, and Li H. 2016. Crustal-scale duplexing beneath the Yarlung Zangbo suture in the western Himalaya. Nature Geosci., 9(7): 555～560.

Garzione C N, Mcquarrie N, Perez N D, Ehlers T A, Beck S L, Kar N, Eichelberger N, Chapman A D, Ward K M, Ducea M N. 2016. The tectonic evolution of the Central Andean plateau and geodynamic implications for the growth of plateaus. Annual Review of Earth & Planetary Sciences, 45(1).

Garzione C N, Molnar P, Libarkin J C, MacFadden B J. 2006. Rapid late Miocene rise of the Bolivian Altiplano: Evidence for removal of mantle lithosphere. Earth and Planetary Science Letters, 241(3-4): 0～556.

Guo L, Zhang H F, Harris N, Xu W C, and Pan F B. 2016. Late Devonian-Early Carboniferous magmatism in the Lhasa terrane and its tectonic implications: Evidences from detrital zircons in the Nyingchi Complex. Lithos, 245: 47～59.

Guo X, Gao R, Zhao J, Xu X, Lu Z, Klemperer S L, and Liu H. 2018. Deep-seated lithospheric geometry in revealing collapse of the Tibetan Plateau. Earth-Science Reviews, 185: 751～762.

Hartley A J, Rice C M. 2005. Controls on supergene enrichment of porphyry copper deposits in the Central Andes: A review and discussion. Mineralium Deposita, 40(5): 515～525.

Hoke G D, Isacks B L, Jordan T E, Blanco N, Tomlinson A J, Ramezani J. 2007. Geomorphic evidence for post-10 Ma uplift of the western flank of the Central Andes (18°30′～22°S). Tectonics, 26: TC5021.

Hou Z, Duan L, Yang Z, Pei Y, Lu Y, McCuaig T C, Zheng Y, Zhu D, Zhao Z, Yang Z. 2015. Lithospheric Architecture of the Lhasa Terrane and Its Control on Ore Deposits in the Himalayan-Tibetan Orogen. Economic Geology, 110: 1541～1575.

Isacks B L. 1988. Uplift of the Central Andean Plateau and bending of the Bolivian Orocline. Journal of Geophysical Research Solid Earth, 93(B4): 3211～3231.

James D E, Sacks S. 1999. Cenozoic formation of the Central Andes: a geophysical perspective. In: Skinner Betal, ed. Geology and Mineral Deposits of Central Andes. Society of Economic Geology, Special Publication, 7: 1～25.

Ji W Q, Wu F Y, Chung S L, Li J X, Liu C Z. 2009. Zircon U-Pb geochronology and Hf isotopic constraints on petrogenesis of the Gangdese batholith, southern Tibet. Chemical Geology, 262: 229～245.

Kley J, Monaldi César R. 1998. Tectonic shortening and crustal thickness in the Central Andes: How good is the correlation? Geology, 26(8): 723～726.

Lamb S, Hoke L, Kennan L. 1997. Cenozoic evolution of the Central Andes in Bolivia and northern Chile. Orogeny Through Time, 121(1): 237～264.

Lamb S, Davis P. 2003. Cenozoic climate change as a possible cause for the rise of the Andes. Nature, 23(425): 792～797.

Lang X H, Liu D, Deng Y, Tang J, Wang X, Yang Z., et al. 2018. Detrital zircon geochronology and geochemistry of Jurassic sandstones in the Xiongcun district, southern Lhasa subterrane, Tibet, China: implications for provenance and tectonic setting. Geological Magazine, 1～19.

Lang X H, Tang J X, Xie F W. 2014. Geological characteristics and exploration potential of the No. III deposit in the Xiongcun district, Tibet, China. Advanced Materials Research, 868: 217～223.

Lee H Y, Chung S L, Lo C H, Ji J Q, Lee T Y, Qian Q, Zhang Q. 2009. Eocene Neotethyan slab breakoff in southern Tibet inferred from the Linzizong volcanic record. Tectonophysics, 477: 20～35.

Li G, Kohn B, Sandiford M, Ma Z, Xu Z. 2018. Post-collisional exhumation of the Indus-Yarlung suture zone and northern Tethyan Himalaya, Saga, SW Tibet. Gondwana Research, 64: 1～10.

Lu Y J, Loucks R R, Fiorentini M L, Yang Z M, Hou Z Q. 2015. Fluid flux melting generated postcollisional high Sr/Y copper ore-forming water-rich magmas in Tibet. Geology, 43: 583～586.

Ma X X, Meert J G, Xu Z Q, Zhao Z B. 2017a. Evidence of magma mixing identified in the Early Eocene Caina pluton from the Gangdese Batholith, southern Tibet. Lithos, 278～281: 126～139.

Ma X X, Xu Z Q, Meert J G, Santosh M. 2017b. Early Jurassic intra-oceanic arc system of the Neotethys Ocean: Constraints from andesites in the Gangdese magmatic belt, south Tibet. Island Arc, e12202.

Ma X X, Meert J G, Xu Z Q, Yi Z Y. 2018. Late Triassic intra-oceanic arc system within Neotethys: Evidence from cumulate appinite in the Gangdese belt, southern Tibet. Lithosphere, 10:

545～565.

Ma Y, Xu Z Q, Li G W, Ma S W, Ma X X, Chen X J, Zhao Z B. 2017. Crustal deformation of the Gandese Cretaceous back-arc basin and formation of Proto-plateau, South Tibet. Acta Petrologica Sinica, 33(12): 3861～3872 (in Chinese with English abstract).

McDermid I R C, Aitchison J C, Davis A M, Harrison T M, M. Grove. 2002. The Zedong terrane: a Late Jurassic intra-oceanic magmatic arc within the Yarlung-Tsangpo suture zone, southeastern Tibet. Chemical Geology, 187: 267～277.

McQuarrie N, Horton B K, Zandt G, Beck S, Decelles P G. 2005. Lithospheric evolution of the Andean fold-thrust belt, Bolivia, and the origin of the Central Andean plateau. Tectonophysics, 399(1-4): 0～37.

Mégard F. 1987. Cordilleran and marginal Andes: a review of Andean geology North of the Aricaelbow (18°S). In: Monger J W H, Francheteau J, eds. Circum-Pacific Belts and Evolufion of the Pacific Ocean Basin. American Geophys. Union, Geodynamic Series, 18: 71～95.

Meng Y K, Xu Z Q, Xu Y, Ma S W. 2018. Late Triassic granites from the Quxu batholith shedding a new light on the evolution of the Gangdese belt in southern Tibet. Acta Geologica Sinica (English Edition), 92: 462～481.

Mo X X, Dong G C, Zhao Z D, Guo T Y, Wang L L, Chen T. 2005. Timing of magma mixing in the Gangdise magmatic belt during the India-Asia collision: zircon SHRIMP U-Pb dating. Acta Geologica Sinica (English Edition), 79(1): 66～76.

Mo X X, Zhao Z D, Deng J F, Dong G C, Zhou S, Guo T Y, Zhang S Q, Wang L L. 2003. Response of volcanism to the India-Asia collision. Earth Science Frontiers, 10(3): 135～148 (in Chinese with English abstract).

de Noblet N, Prentice I C, Joussaume S, Texier D, Botta A, Haxeltime A. 1996. Possible role of atmosphere-biosphere interactions in triggering the lastglaciations. Geoph. Res. Lett., 23(22): 3191～3194.

Pardo-Casas F, Molnar P. 1987. Relative motion of the Nazca (Farallon) and South America plates since Late Cretaceous time. Tectonics, 6: 233～248.

Ramos V A. 2009. Anatomy and global context of the Andes: Main geologic features and the Andean orogenic cycle. In: Kay S M, Ramos V A, Dickinson W R, eds. Backbone of the Americas: Shallow Subduction, Plateau Uplift, and Ridge and Terrane Collision. The Geological Society of America Memoir, 204: 31～65.

Ramos V A, Folguera A. 2009. Andean flat-slab subduction through time. Geological Society London Special Publications, 327(1): 31～54.

Ramos V A. 2009. Anatomy and global context of the Andes: Main geologic features and the Andean orogenic cycle. In: Kay S M, Ramos V A, Dickinson W R, eds. Backbone of the Americas: Shallow subduction, plateau uplift, and ridge and terrane collision, Geological Society of America Memoir, 204: 31～65.

Rodríguez M P, Charrier R, Brichau S, Carretier S, Farías M, Parseval P, Ketcham R A. 2018. Latitudinal and longitudinal patterns of exhumation in the Andes of North-Central Chile. Tectonics, 37(9): 2863～2886.

Royden L. 1996. Coupling and decoupling of crust and mantle in convergent orogens: Implications for strain partitioning in the crust. Journal of Geophysical Research Solid Earth, 101(B8): 17679～17705.

Silver P G, Russo R M, Lithgow-Bertelloni C. 1998. Coupling of South American and African plate motion and plate deformation. Science, 279: 60～63.

Sobolev S V, Babeyko A Y. 2005. What drives orogeny in the Andes? Geology, 33(33): 617～620.

Tafti R, Mortensen J K, Lang J R, Rebagliati M, Oliver J L. 2009. Jurassic U-Pb and Re-Os ages for the newly discovered Xietongmen Cu-Au porphyry district, Tibet, PRC: implications for metallogenic epochs in the southern Gangdese belt. Econ. Geol., 104: 127～136.

Tang Juxing, Wang Denghong, Wang Xiongwu, Zhong Kanghui, Ying Lijuan, Zheng Wenbao, Li Fengji, Guo Na, Qin Zhipeng, Yao Xiaofeng, Li Lei, Wang You, Tang Xiaoqian. 2010. Geological features and metallogenic model of the Jiama copper-polymetallic deposit in Tibet. Acta Geoscientica Sinica, 31(4): 495～506 (in Chinese with English abstract).

Tapponnier P, Xu Z Q, Roger F, Meyer B, Arnaud N, Wittlinger G, Yang J S. 2001. Oblique stepwise rise and growth of the Tibet plateau. Science, 294(23): 1671～1677.

van Hinsbergen D J J, Lippert P C, Li S H, Huang W T, Advokaat E L, Spakman W. 2018. Reconstructing Greater India: Paleogeographic, kinematic, and geodynamic perspectives. Tectonophysics (in press).

Vietor T, Oncken O. 2005. Controls on the shape and kinematics of the central andean plateau flanks: insights from numerical modeling. Earth and Planetary Science Letters, 236(3-4): 0～827.

Wang B, Xie C M, Fan J J, Wang M, Yu Y P, Dong Y C, Hao Y J. 2019. Genesis and tectonic setting of Middle Permian OIB-type mafic rocks in the Sumdo area, southern Lhasa terrane. Lithos, 324～325: 429～438.

Wang C, Ding L, Zhang L Y, Ding X L, Yue Y H. 2018. Early Jurassic high-Mg andesites in the Quxu area, southern Lhasa terrane: Implications for magma evolution related to a slab rollback of the Neo-Tethyan Ocean. Geological Journal, 1～17.

Wang C, Ding L, Zhang L Y, Kapp P, Pullen A, Yue Y H. 2016. Petrogenesis of Middle-Late Triassic volcanic rocks from the Gangdese belt, southern Lhasa terrane: Implications for early subduction of Neo-Tethyan oceanic lithosphere. Lithos, 262: 320～333.

Wang E C, Kamp P J, Xu G, Hodges K V, Meng K, Chen L, Wang G, Luo H. 2015. Flexural bending of southern Tibet in a retro foreland setting. Scientific reports, 5, 12076.

Wang H Q, Ding L, Cai F L, Xu Q, Li S, Fu J J, Lai Q Z, Yue Y H, Li X. 2017. Early Tertiary deformation of the Zhongba-Gyangze Thrust in central southern Tibet. Gondwana Research, 41: 235～248.

Wang J G, Hu X M, Garzanti E, An W, Liu X C. 2017. The birth of the Xigaze forearc basin in southern Tibet. Earth and Planetary Science Letters, 465: 38～47.

Wen D R, Liu D Y, Chung S L, Chu M F, Ji J Q, Zhang Q, Song B, Lee T Y, Yeh M W, Lo C H. 2008. Zircon SHRIMP U-Pb ages of the Gangdese Batholith and implications for Neotethyan subduction in southern Tibet. Chemical Geology, 252: 191～201.

Xu Z Q, Wang Q, Pêcher A, Liang F H, Qi X X, Cai Z H, Li H Q, Zeng L S, Cao H. 2013. Orogen-parallel ductile extension and extrusion of the Greater Himalaya in the late Oligocene and Miocene. Tectonics, 32: 191～215.

Xu Z Q, Wang Q, Li Z H, Li H Q, Cai Z H, Liang F H, Dong H W, Cao H, Chen X J, Huang X M, Wu C, Xu C P. 2016. Indo-Asian collision: Tectonic transition from compression to strike slip. Acta Geologica Sinica, 90(1): 1～23 (in Chinese with English abstract).

Xu Z Q, Wang Q, Sun W D, Li Z H. 2018. The spherical structure of the Earth and across-sphere tectonics. Geological Review, 64(2): 261～282 (in Chinese with English abstract).

Yang J, Xu Z, Li Z, Xu X, Li T, Ren Y, Li H, Chen S, Robinson P T. 2009. Discovery of an eclogite belt in the Lhasa block, Tibet: A new border for Paleo-Tethys? Journal of Asian Earth Sciences, 34(1): 76～89.

Yang Z M, Lu Y J, Hou Z Q, Chang Z S. 2015. High-Mg diorite from Qulong in southern Tibet: Implications for the Genesis of adakite-like intrusions and associated porphyry Cu deposits in collisional orogens. Journal of Petrology, 56: 227～254.

Yuan X, Sobolev S, Kind R. 2002. Moho topography in the central Andes and its geodynamic implications. Earth Planet. Sci. Lett., 199: 389～402.

Yin A, Harrison T M. 2000. Geologic evolution of the Himalayan-Tibetan orogen. Annual Review of Earth and Planetary Sciences, 28: 211～280.

Zhang C, Bader T, van Roermund H, Yang J, Shen T, Qiu T, Li P. 2018. The metamorphic evolution and tectonic significance of the Sumdo HP-UHP metamorphic terrane, central-south Lhasa Block, Tibet. Geological Society, London, Special Publications, 474.

Zhu D C, Wang Q, Zhao Z D, Chung S L, Cawood P A, Niu Y, Liu S A, Wu F Y, Mo X X. 2015. Magmatic record of India-Asia collision. Scientific reports, 5: 14289.

Ziabrev S V, Aitchison J C, Abrajevitch A V, Badengzhu, Davis A M, Luo H. 2004. Bainang Terrane, Yarlung-Tsangpo suture, southern Tibet (Xizang, China): a record of intra-Neotethyan subduction-accretion processes preserved on the roof of the world. Journal of the Geological Society, London, 161: 523～538.

参　考　文　献

马元，许志琴，李广伟，马士伟，马绪宣，陈希节，赵中宝. 2017. 藏南冈底斯白垩纪弧后盆地的地壳变形及初始高原的形成. 岩石学报，33(12):3861～3872.

唐菊兴，王登红，汪雄武，钟康惠，应立娟，郑文宝，黎枫佶，郭娜，姚晓峰，李磊，王友，唐晓倩. 2010. 西藏甲玛铜多金属矿床地质特征及其矿床模型. 地球学报，31(4)：495～506.

许志琴，王勤，李忠海，李化启，蔡志慧，梁凤华，董汉文，曹汇，陈希节，黄学猛，吴婵，许翠萍. 2016. 印度-亚洲碰撞：从挤压到走滑的构造转换. 地质学报，90(1)：1～23.

许志琴，王勤，孙卫东，李忠海. 2018. 地球的层圈结构与穿越层圈构造. 地质论评，64(2)：261～282.

From Andean orogen to Gangdese orogeny: from ocean continent subduction to continent-continent collision

XU Zhiqin*[1)], ZHAO Zhongbao[2)], MA Xuxuan[2)], CHEN Xijie[2)], MA Yuan[2)]

1) *School of Earth Sciences and Engineering, Nanjing University, Nanjing*, 210046;

2) *Institute of Geology, Chinese Academy of Geological Sciences, Beijing*, 100037

* *Corresponding author*: 3077864156@*qq.com*

Abstract

The global orogenic system can be divided into two main types: accretionary type and collisional type. Nowadays, studies of two giant orogenic systems on the Earth shows that 1) the accretionary orogenic system are happening around the Pacific Ocean by oceanic plates subducted beneath continental plates, and 2) the Himalayan collisional orogenic system has entered the stage of continent-continent collision after oceanic plate-continental subduction. Among them, the Andean orogenic belt is a typical "Andean island arc belt" and "Andean-Cordillera subduction related accretionary orogenic system" which characterized by "deep (steep)-shallow (flat) alternating subduction of the oceanic plate, oceanic island-continent accretional collision and subduction induced plateau uplift" that formed by the multi-stage subduction of the Lazaca oceanic plate in the eastern Pacific Ocean. The Gangdese orogeny belt, located in the interior of the Asian continent, underwent two mainly orogenic stages. The first stage is represented by northward oceanic plate subduction, while subduction accompanied closure of the Neo-Tethys oceanic basin. This stage includes forming the multi-oceanic islands in the Neo-Tethys, which probably initiated in the early Mesozoic, and multi-stages subduction and convergence between the Lhasa terrane and oceanic islands. That results in the accretion and collision of the oceanic islands and the Lhasa terrane which lead to form the Gangdese magmatic arc and is similar to the Andean-type subduction-accretion orogenic system. Meanwhile, initial Gangdese Plateau may develop during the magma eruption and transformation from subduction to collision. In the early Cenozoic, the Gangdese orogeny belt entered the second stage of continent-continental collision between Indian and Asian continents. Then it formed large-scale E-W trending thrust faults, strike-slip faults and S-N trending rift systems. Therefore, the Andean orogeny belt is the geological history of the Gangdese orogeny evolution, current Gangdese orogeny belt is the future geology of the Andean orogenic belt. Aim to study the tectonic evolution of Gangdese orogeny belt, especially the early tectonic magmatic activity, we must compare the geological evolution of the Andean subduction and accretion process.

Key words: Orogenic types; Andean orogenic belt; Gangdese orogenic belt